

## Introduction and Application of Rotational Abrasion Device to Determine Concrete Pavement Abrasion

Jalal Kamali, M.H.<sup>1</sup>, Hassani, A.<sup>2\*</sup> and Sodagari, J.<sup>3</sup>

<sup>1</sup> Ph.D. Candidate in Highway Engineering, Tarbiat Modares University, Tehran, Iran.

<sup>2</sup> Professor in Highway Engineering, Tarbiat Modares University, Tehran, Iran.

<sup>3</sup> Part-Time Lecturer, Tarbiat Modares University, Tehran, Iran.

Received: 30 Sep. 2018;

Revised: 26 Jan. 2019;

Accepted: 13 Feb. 2019

**ABSTRACT:** Abrasion susceptibility of highway pavements has a great impact on the skid resistance, and consequently accident rate. A rotational abrasion device is introduced, providing the advantage of field simulation of wheel passage, in comparison with existing standard methods. The device was used to measure abrasion susceptibility of concrete pavements with different textures. The obtained results were evaluated using the standard Wide Wheel Abrasion Test. It is shown that there is a good conformity between abrasion rates acquired from the two tests. The results also show that negative textures, such as grooving, lead to a highly variant unreliable outcome in Wide Wheel Abrasion Test. The brushed samples (perpendicularly or parallelly brushed) underwent the highest abrasion level due to high interaction between texture and wheel (the average final measured abrasion amount is 90% more in brushed samples compared to non-textured samples). Since Rotational Abrasion Test is able to apply extensive loading, its results, as compared to the other test, is not susceptible to random surface protuberances or cavities (burlap dragged and grooved samples).

**Keywords:** Abrasion Resistance, Concrete Abrasion, Concrete Macrotecture, Rotational Abrasion Test, Wide Wheel Abrasion Test.

### INTRODUCTION

According to official records of Iranian Legal Medical Organization in 2017, more than 16200 people lost their lives in road accidents in Iran (Iranian Legal Medical Organization, 2017). In a research on casualties caused by accidents in Iran, Rasouli et al. (2008) showed that death toll rates of the accidents have increased from 22.1 in 1997 to 40.5 per 100,000 people in 2005, which categorizes Iran as a high-risk country in the area of road accidents (Rasouli et al., 2008).

For any life lost in road accidents brings about huge loss to the country's economy, which was estimated to be 8530 million Rials (244,000 USD) per person for the country, in 2012 (Jalal Kamali, 2012). Several studies have been carried out on the relationship between friction coefficient of pavement surface and road accidents, all of which proved that increasing the friction coefficient improves road safety. For example, in a study performed on the relationship between friction and the rate of accidents in Sweden, it was found that an increase in pavement

\* Corresponding author E-mail: hassani@modares.ac.ir

friction significantly reduces the rate of accidents. The results of the research are presented in Table 1 (Wallman et al., 2001).

Even though the determination of contribution of pavement friction and skid resistance on the rate of accidents is complicated, some researches are conducted on their relationships. For instance Xiao et al. (2000) showed the safety condition, measured by the reduction rate in wet pavement crashes, could be improved nearly 60% if the skid number increased 44%.

**Table 1.** Variations of the rate of accidents with respect to changes in friction coefficient (Wallman et al., 2001)

Accidents rate (Accidents per million vehicle-kilometers)	Friction coefficient range
0.80	< 0.15
0.55	0.15 - 0.24
0.25	0.25 - 0.34
0.2	0.35 - 0.44

Four important factors affecting the friction between the road surface and vehicle tires include surface specifications, vehicle performance specifications, tire characteristics and environmental conditions (Wu et al., 2012, Jalal Kamali et al., 2013), among which, surface specifications are within the scope of highway engineering.

In tribology, abrasion is the process by which relative motion between a surface and hard particles or protuberances on an opposing surface produces abrasive wear of that surface (ASTM G40-15). Abrasion is usually measured by the weight loss of the material during the abrasive process. Surface frictional specifications, on the other hand, consist of various surface parameters (e.g. texture, skid resistance and coefficient of friction), and are measured using different test methods and apparatus (e.g. Sand Patch Test, British Pendulum Test and Dynamic Friction Tester).

Several studies have investigated the

effect of abrasion on surface frictional specifications. Wang et al. (2014) conducted a research and counted the abrasion of an asphalt pavement surface as one of the factors affecting friction and presented a model for predicting skid resistance of the surface of the pavement, where this model was dependent on initial skid resistance of surface and some time-dependent factors. Their result showed that the concrete surface friction (measured by British Pendulum Tester) is significantly dependent on the duration that samples have undergone abrasion.

In another study, performed on the hot mix asphalt, it was determined that International Friction Index (IFI) drops with an increase in the number of abrasion cycles, where the IFI may even drop by up to 60% depending on the type of aggregate and mix design (Kassem et al., 2013).

Another study was performed on the effect of fly ash on the abrasion resistance of concrete surfaces. In the majority of specimens, in wet conditions, as the duration of abrasion increases, the British Pendulum Number decreases (Yoshitake et al., 2016).

Another study investigated the abrasion resistance of rockfill material as an important parameter affecting the material behaviour. They were assessed an experimental correlation between Los Angeles Abrasion Value and internal friction angle of the material (Ghanbari et al., 2013).

In a study performed on the impact of Nanomaterials on the abrasion resistance of concrete pavements, it was shown that both micro and macro textures have significant impacts on the surface friction. This research focused on the need for creating macrotexture with high resistance against abrasion and it has been stated that resistance of macrotexture against abrasion can lead to a reduction in the cost related to providing friction during pavement maintenance process (Gonzalez et al., 2014).

There are a few standardized test methods

to quantify abrasion susceptibility of concrete surfaces, which are different in some features (ASTM C779, 2012, Purwanto and Arni priastiwi, 2012, GB/T16925, 1997, ASTM C1138, 2012, ASTM C944, 2012). Considering contact type, some perform rubbing to simulate abrasion progress (e.g. ASTM C779 – Procedure A, BS EN 1338 – Wide Wheel Abrasion Test and Böhme Test, and GB/T16925), while the others implement rolling action (e.g. ASTM C779 – Procedure B and C, and ASTM C944). Simulating real conditions, as another feature, is implemented in some standards by utilizing wheel passage (e.g. BS EN 1338 – Wide Wheel Abrasion Test). Other tests evaluate the effect of different objects, such as disk, needle, ball bearing, etc., on the surface abrasion (e.g. ASTM C779, ASTM C1138, ASTM C944, and GB/T16925).

Numerous studies have been conducted to evaluate concrete abrasion, using the mentioned standard test methods. Yet, amongst them, some remarkable researches can be noticed. In a study performed on the abrasion resistance of high-performance concrete utilizing ASTM C1138, a mathematical model has developed which correlate abrasion resistance as a function of time and load in a non-linear manner (Horszczaruk, 2008). In another research conducted on the abrasion resistance of high-strength concrete using the same standard, it was indicated that the abrasion resistance of high-strength concrete depends on compression strength, modulus of elasticity, fiber material and dimensions (Horszczaruk, 2005). Li et al (2006) investigate the abrasion resistance of concrete pavement containing nano-particle utilizing GB/T16925 standard. They declare that abrasion resistance of concrete containing nanoparticles are much higher than that of concrete containing polypropylene fiber. They also reported that increasing the compressive strength of concrete result in more abrasion resistance of

concrete pavements (Li et al., 2006).

Besides, miscellaneous testing methods have been employed in various studies to evaluate concrete abrasion properties. In these studies, new test methods are introduced in order to simulate a specific condition, or to improve the existing procedures. Adewuyi et al. (2017) used BS EN-1338 procedure to examine the abrasion susceptibility of concrete samples. However, abrasion depth was collected as the measured parameter, despite the standard procedure. Rafat (2013) used the test device, introduced in BS EN-1338, to perform a totally different test procedure. García et al. (2012) also conducted a research on surface abrasion, using the same standard. However, abraded depth variation was measured to compare abrasion resistance of the samples.

Surface finishing of concrete pavements usually leads to a smooth surface. Therefore, leaving the untextured surface to be the final surface of the pavement, causes many safety problems due to lack of adequate friction. Implementing a suitable texturing procedure, generates enough macrotexture and consequently, skid resistance. Many factors need to be considered to choose the type of pavement macrotexture, such as traffic characteristics, type and gradation of aggregates, weather conditions, pavement surface noise, and the required skid resistance (Hall et al., 2009).

Depth, spacing and orientation of pavement macrotexture have significant impacts on frictional properties, noise production and ride quality (Ardani, 2006). Direction of the required macrotexture depends on the application and function of pavement. Longitudinal textures are more efficient on cross slopes and horizontal curves, while, transverse textures are more resistant against head-on skidding. Besides, due to the existence of cross slope, transverse texture provides better drainage, reducing the probability of the hydroplaning phenomenon

Different procedures can be employed to create macrotexture on a concrete pavement. The most commonly used ones are (ACI, 1997, Ahammed and Tighe, 2008);

- Dragging artificial turf transversally and longitudinally on fresh concrete
- Longitudinal or transversal brushing on fresh concrete
- Longitudinal or transverse brooming on fresh concrete
- Burlap dragging on the surface of fresh concrete
- Grooving or grinding the hardened concrete
- Longitudinal or transverse tinning
- Exposed aggregate

Since the mentioned abrasion measurement methods are not modelling the real abrasion in field it seems necessary to design a testing procedure capable of modelling a more realistic condition. Besides in the above mentioned researches, most of the abrasion measurement devices are not available or too costly in Iran so in this research a testing device with a better simulation capability and less expenses is introduced.

## **OBJECTIVES AND RESEARCH OUTLINE**

The main goal of current research was to introduce and evaluate the new rotational abrasion measurement device. A comparison with another standard abrasion test method was considered to validate the new device results. The other objective was to determine the abrasion resistance of various pavement surface macro-textures.

The pavement samples, textured through different methods, are tested to determine abrasion rate, using Rotational and Wide Wheel Abrasion tests. Afterward, statistical analyses are carried out and data were clustered considering various aspects such as loading amplitude and repetition, and texture

type. Eventually, the trends of different types of textures, are discussed.

## **LABORATORY PROCEDURE**

In this section the Rotational Abrasion Device is briefly described. Afterwards material properties and laboratory procedures such as concrete mixture design, sample preparation, texture creation and abrasion tests have been briefly described in this section.

### **Rotational Abrasion Device**

The rotational abrasion device is originally inspired by traffic simulators, in a smaller scale. This device is registered under the patent number of 89/A29675 in Iran. The overall view of the device have been showed in Figure 1.

The rotational abrasion device consists of two arms holding the steel wheels. The arms are rotated by a transmission system with controllable speed, which can reach a maximum speed of 30 rpm. The force exerted by each wheel is adjustable by two springs mounted on it, and can be measured using a weighing sensor under the wheel. The loading system, illustrated in Figure 1, can apply a maximum load of 450 by each wheel.

The pavement samples are shaped like a square toroid section. The samples mold is illustrated in Figure 2 in each test run, eight samples are placed and fixed in the device to undergo abrasion induced by wheel passage.

### **Aggregates**

Coarse and fine aggregates used in the concrete mixture were all supplied from a mine, located in the southwest of Tehran. The following conventional tests are performed on aggregates and the results are acquired.

- Mechanical properties: Abrasion resistance of the aggregates are determined by Los Angeles Abrasion Test. The impact resistance for coarse-grained aggregates has

been also achieved by Aggregate Impact Value Test. The results are presented in Tables 2 and 3.

- Aggregate soundness: Weight loss values of the aggregate, obtained in Soundness Test using magnesium and sodium sulfate have been presented in Table 4.

Coarse-grained aggregates grading curves

have been obtained, considering the upper and lower limits of ACI regulation. Since the fine-grained aggregates gradation, is within the required limits, no further gradation is needed. Figure 3 shows gradation diagram of the fine grained and coarse grained aggregates used for concrete mixture.

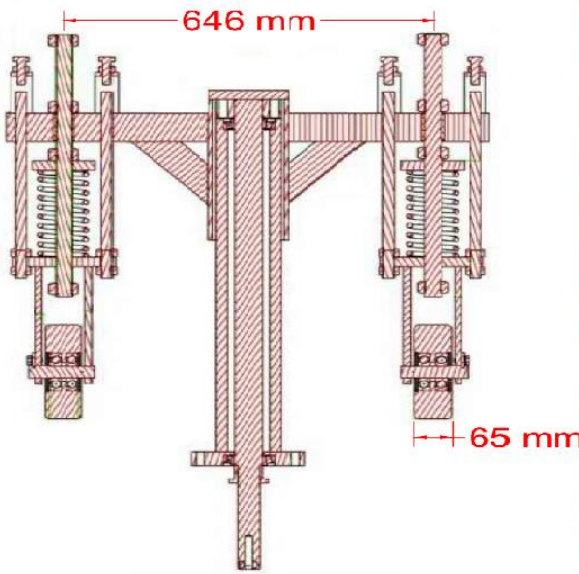


Fig. 1. Overall view of the rotational abrasion device

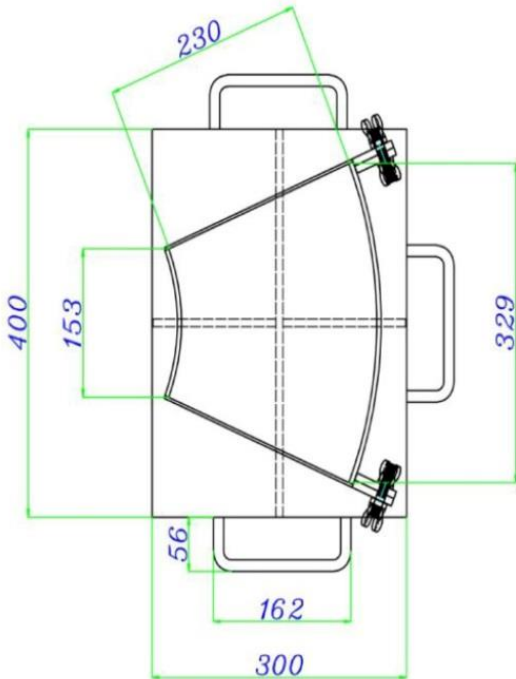


Fig. 2. Molds used to prepare pavement samples of rotational abrasion device (dimensions are given in mm)

**Table 2.** Specifications of fine and coarse aggregates

Variables	Standard code	Coarse aggregate	Fine aggregate
Specific gravity (g/cm <sup>3</sup> )	ASTM C136	2.67	2.67
Bulk Specific gravity (g/cm <sup>3</sup> )	ASTM C29	1641.4	-
Water absorption in SSD (%)	ASTM C127	1.3	2.6
Fineness modulus	ASTM C136	-	2.85
Sand Equivalent (%)	ASTM D2410	-	80

**Table 3.** Abrasion and impact resistance tests of coarse aggregates

	Los Angeles abrasion test	Impact resistance value
Loss of weight (%)	12	8.1

**Table 4.** Results of coarse aggregate soundness test

	Soundness test	Weight loss
Coarse-grained aggregates	With sodium sulfate	9.5%
	With magnesium sulfate	12.6%

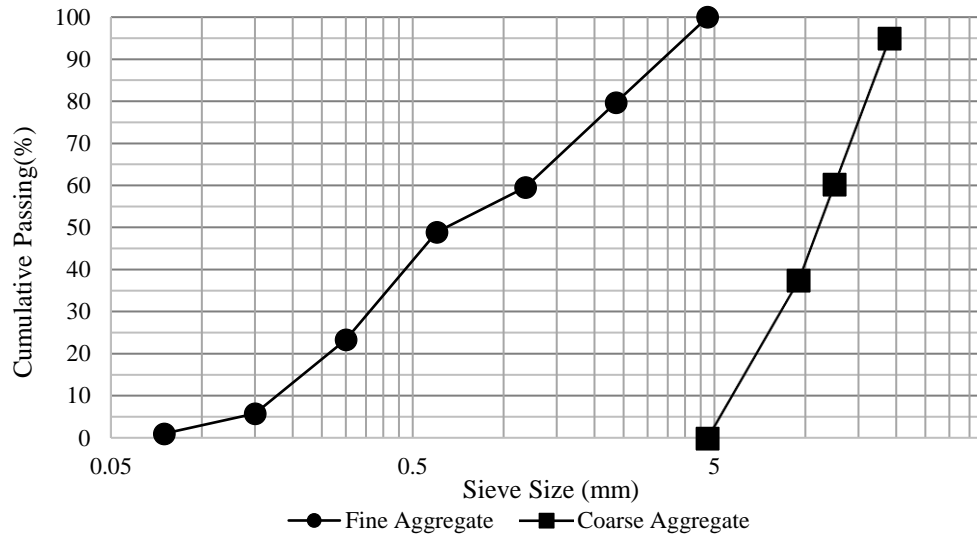


**Fig. 3.** Gradation diagram for fine-grained and Coarse-grained aggregates

### Cement

Physical and chemical properties of the cement were assessed and the results are reported in Tables 5 and 6.

### Concrete Mix Design

The concrete mix design is determined according to ACI-211 regulation. Considering the molds dimensions (presented in Figure 2, with a height of 10 cm), the size of the largest used aggregate was chosen  $\frac{3}{4}$  inch. Since, the results of this research may be used in field, the designed concrete specifications need to be similar to conventional constructed pavement

concretes. Therefore, minimum compressive and flexural strength of concrete in the design process were considered to be 40 and 4.5 MPa, respectively (Delatte, 2014). Moreover, the slump value was assumed to be between one and two inches. Concerning the properties of aggregates and expected specifications of the concrete, a primary mixture design was achieved. After several modifications, the final mixture proportions was determined, presented in Table 7.

### Preparation of Specimens

The specimens were constructed as designed, and later on, textured by different

methods. As stated before, these texturing procedures are the most commonly used methods to create macrotexture on concrete pavements. Afterwards the specimens were emerged in the water for 28 days to be cured. The following symbols are going to be used to indicate different types of macrotexture:

- Without texture (No Texture): N.T.
- Texture created by dragging artificial turf (Turf Dragging): T.D.
- Texture created by grooving (Grooving): G.
- Texture created by dragging plastic brush parallel to traffic path (Parallel Brushing): Par.B.
- Texture created by dragging plastic brush perpendicular to traffic path (Perpendicular Brushing): Per.B.
- Texture created by dragging burlap parallel to traffic path (Burlap Dragging): B.D.

**Rotational Abrasion Test**

The concrete samples were weighed and placed and fastened inside the Rotational Abrasion Test device. The test was run using different loads, and the abrasion was measured during time. The impact of traffic variation was evaluated by two factors: load and iteration. The applied loads were selected between 120 and 360 kg. The samples were weighed at specific load cycles: 100, 200, 400, 600, 800 and 1000. The load magnitude

and passage iteration were selected using experimental design methods. The abrasion value is determined as the weight loss ratio (i.e. the ratio of the specimen weight loss to its initial weight) in each of the aforementioned cycles.

**Wide Wheel Abrasion Test**

In this research, the Wide Wheel Abrasion Test was performed according to the BS EN 1338:2003 Standard, to abrade the differently textured concrete specimens. The test device abrades the surface of concrete specimens, in the vicinity of a steel wheel, and in the presence of Alumina Fused (corundum, Al<sub>2</sub>O<sub>3</sub>).

After the concrete sample is abraded for one minute, the dimensions of the abraded trace, left by the wheel, was measured accurately, as required in the standard. In this research, in order to increase the accuracy and also to facilitate the measurement of dimensions of the created groove, a high-quality photo was taken from the surface of the specimen. Dimensions of the wheel track were then measured, using image processing software. Moreover, the specimens were wetted before imaging, to enhance the abraded area contrast and make it well defined in the photos. Figure 4 depicts a concrete specimen, textured by dragging artificial turf on fresh concrete, after performing the test.

**Table 5.** Physical and mechanical specifications of the used cement

	<b>Specific surface</b>	<b>Specific gravity</b>	<b>3 Days compressive strength</b>	<b>7 Days compressive strength</b>
Minimum requirement	-	-	12 MPa	19 MPa
Cement	3250 cm <sup>2</sup> /gr	3.15 gr/cm <sup>3</sup>	12.5 MPa	21.9 MPa

**Table 6.** The chemical composition of the cement

<b>Component</b>	<b>L.O.I</b>	<b>CaO</b>	<b>Si<sub>2</sub>O</b>	<b>Al<sub>2</sub>O<sub>3</sub></b>	<b>Fe<sub>2</sub>O<sub>3</sub></b>	<b>SO<sub>3</sub></b>	<b>MgO</b>	<b>K<sub>2</sub>O</b>	<b>Ti<sub>2</sub>O</b>	<b>Cl</b>	<b>Total</b>
Weight (%)	1.85	62.208	18.492	4.026	3.777	3.208	2.731	0.811	0.366	0.173	97.642

**Table 7.** Concrete mix design

	<b>Gravel (kg/m<sup>3</sup>)</b>	<b>Sand (kg/m<sup>3</sup>)</b>	<b>Cement (kg/m<sup>3</sup>)</b>	<b>Water (kg/m<sup>3</sup>)</b>	<b>W/C ratio</b>
Mix design proportion	1091	670	400	176	0.44

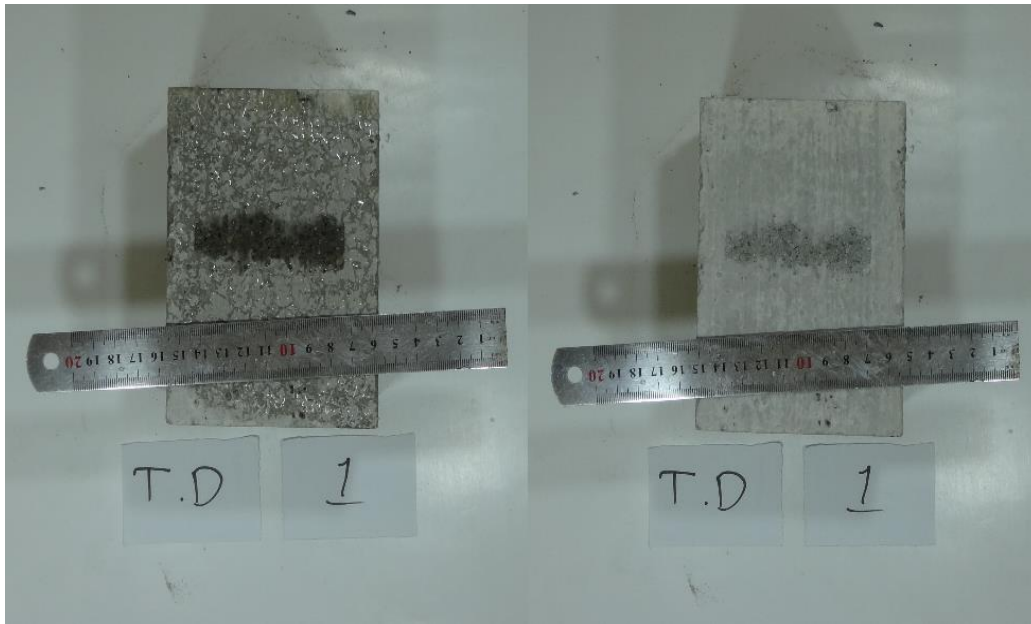


Fig. 4. Images taken from a wide wheel abraded sample, in wet and dry states

## RESULTS AND DISCUSSIONS

### Rotational Abrasion Test

Figure 5 illustrates the abrasion values of various samples under the loading amplitude of 200 kg. As it can be followed in the figure, N.T samples have the lowest abrasion values, and other samples are ordered, from low to high abrasion value, as B.D, T.D, Par.B, Per.B, and G. The abrasion results, under other loading amplitudes (120, 280 and 360 kg) provided the same trend.

It can be clearly seen in the Figure 5 that abrasion rate is descending as loading continues. The abrasion trend is rather similar for all samples, except G, and can be explained in two parts:

- From the beginning of the test till the 200<sup>th</sup> cycle;
- The rest of the test (from 201<sup>st</sup> cycle till the end of the test).

The abrasion rate in the first part is nearly 8 times higher than the second part abrasion rate. Such variation in abrasion rate may be a result of following factors:

- The integrity loss of concrete surface caused by texturing, flaws its strength. As a result, in the first part, the newly textured

surface undergoes high abrasion. As loading continues, the created texture wears away gradually, leaving a worn down intact surface. Therefore, in the second part, the worn surface, experiences less abrasion under wheel loading. This theory is strongly supported, considering the parallel abrasion trend of differently textured samples, in the second part (after 200<sup>th</sup> cycle). The abrasion trends, in the second part, are parallel because all the samples are worn away and an intact surface is being loaded.

- After the fresh concrete was textured, a plastic cover was placed on the samples to trap the moisture for 24 hours (before water-submerged curing), however, the surface layer may yet lose water through evaporation. The lost moisture in the surface layer negatively affects strength gaining process in the first day. During the abrasion test, after the surface layer is worn away, the remaining surface is more abrasion resistant. This process is the other explanation for the abrasion trends. Since N.T conforms similar trend while it is not textured, the latter explanation can be accounted as the main reason.

However, the abrasion behavior in G

samples is rather different. The abrasion rate, in G samples, is ascending, as the others are. Yet, as loading continues, despite the relative decrease, the abrasion rate is more ascending compared to the others. A detailed evaluation of the G samples, during the abrasion process, revealed that the weight loss of the specimens

is not completely due to abrasion process. Indeed, some of the weight loss was a result of fracture occurrence at grooves edges. The ground look on a G sample, depicted in Figure 6 confirms that abrasion is not the only procedure affecting the surface.

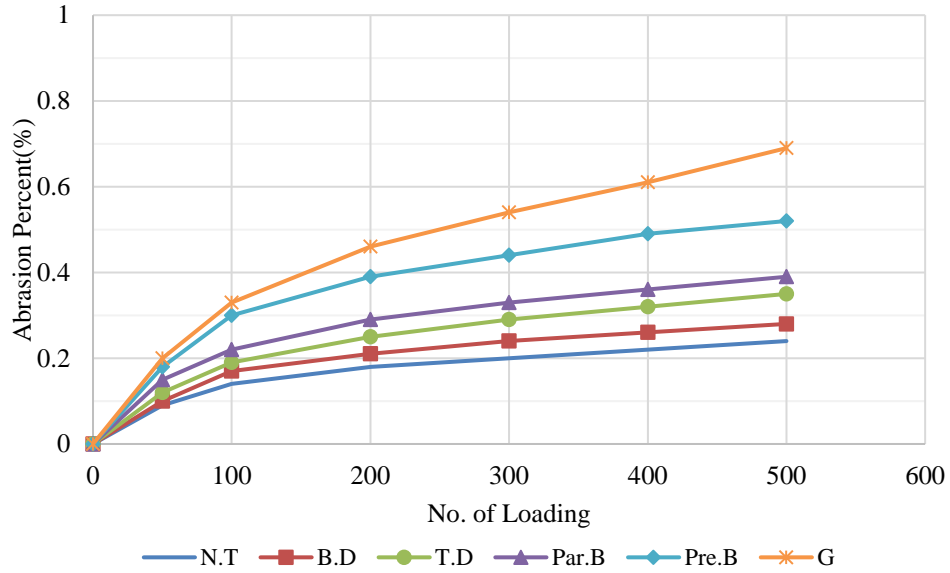


Fig. 5. Abrasion values of textured samples, tested under 200 kg loading

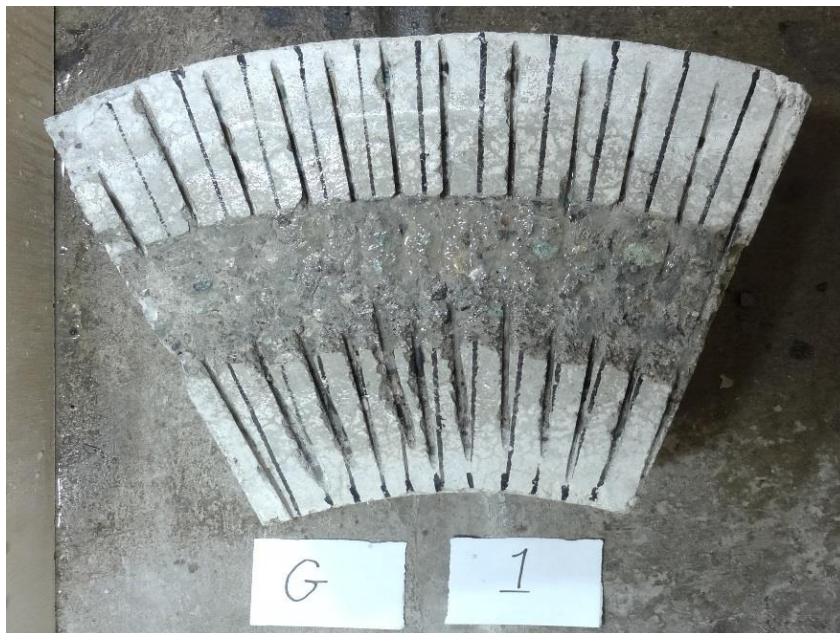


Fig. 6. Grooved sample, after performing Rotational Abrasion Test (dimensions of the specimen can be found in Figure 2)

Figure 7 presents a comparison of the abrasion results under different loading intensities, for the six different textures, implemented on concrete surface. As it could be predicted, the abrasion values of all different textures increases as the loading amplitude increases. The increasing rate, however, is different for the texture type G, compared to the other types. For all the

samples except G, the rate of abrasion intensification, decreases as the loading amplitude increases, while for the sample type G the rate increases with the increase of loading amplitude. This is mainly due to the fact that the weight loss in sample type G is not only a result of abrasion process, but also a consequence of grooves edge fracture.

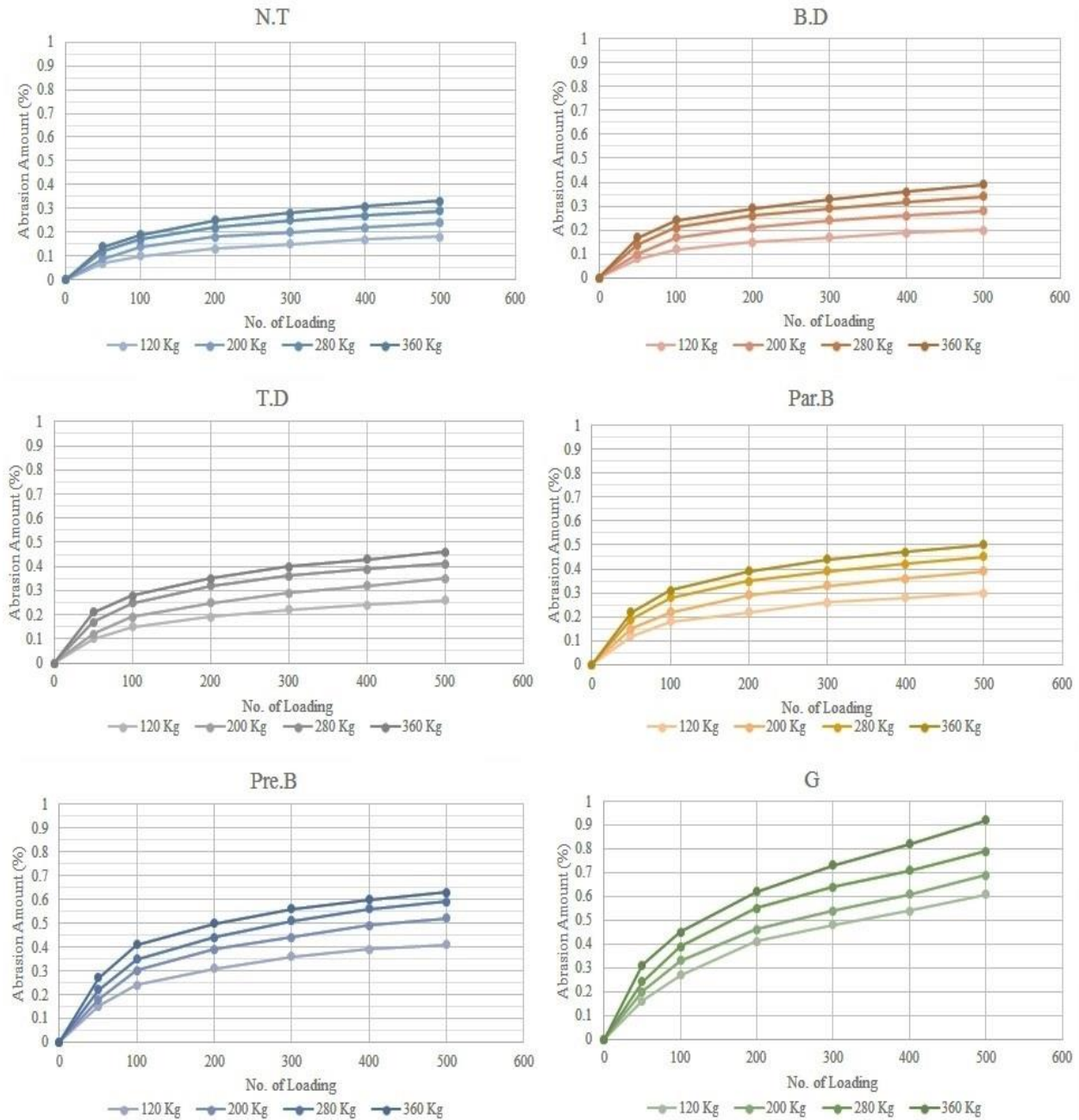


Fig. 7. Variation of abrasion values versus loading amount and texture type

### Wide Wheel Abrasion Test

The images acquired from specimens after Wide Wheel Abrasion Test were digitally processed to achieve Abrasion Index. Abrasion Index is defined as the abraded width described in BS EN-1338:2003. The results are presented in Figure 9. The corresponding analysis of variance has also been acquired in Table 8 in order to evaluate the statistical status of the experimental results. The F-statistic and sig. values in Table 8 indicate the significance of the discrepancies among the AI of different textures. As it can be noted in ANOVA, the

standard deviation of samples G is significantly higher, which indicates the high results variations and lack of reliability compared to the others. Such variations between G results is due to the variation of testing condition, especially where exactly the wheel touches the sample. If the wheel is placed on the groove, the abrasion rate increases due to a tighter engagement between the wheel and concrete in presence of the abrasive powder. A possible placement of the wheel trace in comparison to grooves has been illustrated in Figure 8.

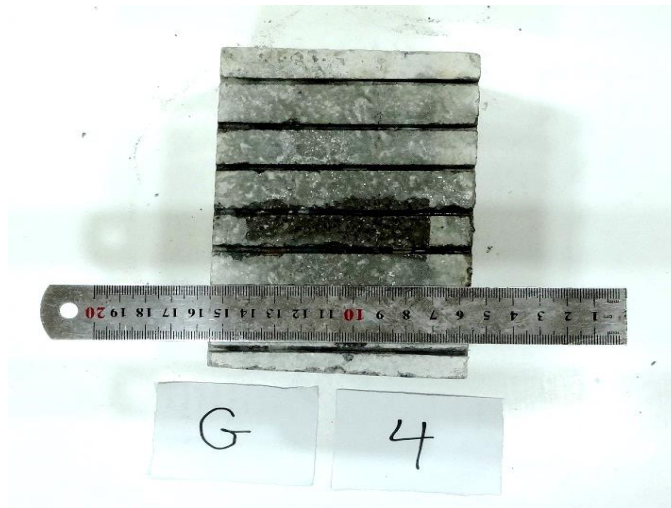


Fig. 8. Grooved sample after employing Wide Wheel Abrasion Test

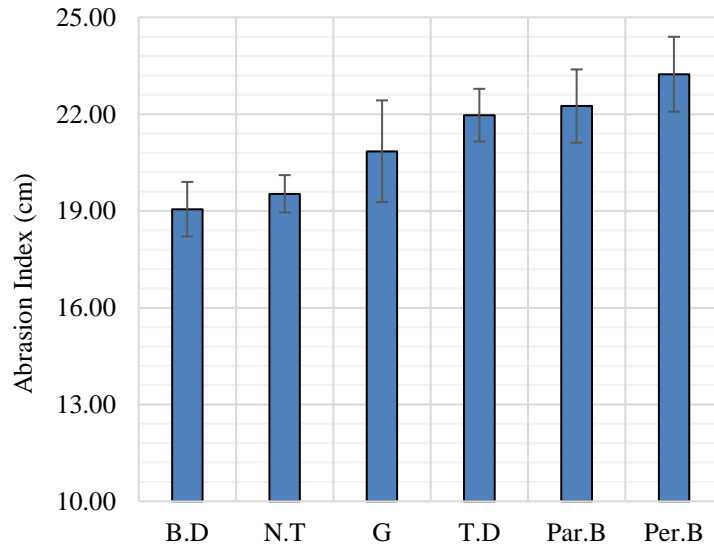


Fig. 9. Grooved sample after employing Wide Wheel Abrasion Test

**Table 8.** Analysis of variances of Wide Wheel Abrasion Test results

	<b>T.D.AI</b>	<b>G.AI</b>	<b>N.T.AI</b>	<b>B.D.AI</b>	<b>Per.B.AI</b>	<b>Par.B.AI</b>
Mean	21.9670	20.9032	19.5310	19.0543	23.2355	22.2490
N	23	19	21	21	22	21
Std. Deviation	0.83549	1.61961	0.59415	0.86678	1.18787	1.16557
	<b>Sum of squares</b>	<b>df</b>	<b>Mean square</b>	<b>F</b>	<b>Sig.</b>	
Between groups	285.252	5	57.050	40.056	0.000	
Within groups	172.335	121	1.424			
Total	457.587	126				

### Comparative Analysis of the Abrasion Tests

Comparing the abrasion results, obtained from Rotational and Wide Wheel Abrasion Tests reveals some certain conformities. Excluding the sample type G, the results of the conducted tests follow a similar sequence, with respect to abrasion rate. The descending order of the abrasion amount in Rotational Abrasion Test would be Per.B, Par.B, T.D, B.D, and N.T. For the Wide Wheel Abrasion Test, the latter two types (B.D and N.T) are approximately equal in results, but the B.D abrasion index is less.

Considering the abrasion mechanism in the employed abrasion devices, it is clear that the abrasion rate is directly affected by the impact frequency and intensity between the wheel and the surface. For a specific type of pavement, textures causing higher impact frequencies and/or intensities, will certainly undergo higher abrasion under traffic loading. Since, a negatively textured surface with a specific frequency of protuberances provides less impact intensity, in comparison with a similar positively textured surface, it is less vulnerable to abrasion. However, grooved samples results proved that negative textures, may result in higher rate of weight loss, due to the fracture of grooves edges. Negative texture is defined as a texture in which the majority of the surface is on a higher level than the grooves made as the texture.

Besides, for negative textures, the wheel placement position on the surface in Wide Wheel Abrasion Test is a determinant factor in abrasion rate. With regard to the stated difficulties, it can be concluded that, for

negative textures, the employed testing methods cannot yield reliable results, as discussed before.

The result of the sample type B.D (i.e. burlap dragged specimens) in Wide Wheel Abrasion Test, showed the lowest abrasion value which violates the trend, achieved by Rotational Test. Since in Wide Wheel Abrasion Test the wheel touches a limited area on the sample, and also the test duration is quite short, random protuberances on the surface are relatively determinant in the result.

During burlap drag, on the fresh concrete surface, the burlap tissue may trap the aggregates and pull them out, causing random protuberances on the pavement surface. During the 60 seconds testing time, if the wheel is placed on a pulled out aggregate, it cannot abrade the sample properly. Therefore, the Wide Wheel Abrasion Test may not yield reliable results from the samples which have random protuberances on the surface. The rotational test, in contrast, can afford reliable results, due to the loading conditions including duration, load amplitude, and extensive loading.

The sample type G does not seem to yield consistent results in either test. This can be indicated through variance analysis and sample inspections. A considerable distinction between sample type G and other sample types is that the former is textured negatively. The negativeness of textures, with the applied intervals of sample type G (2.5 cm), results in a low reliability of Wide Wheel Abrasion Test outcome. This owes to the fact that the wheel is less like to engage

the negative textures. The test is, also, indifferent to the texture specifications such as shape (rectangular or triangular) and depth.

## CONCLUSIONS

In this research, the Rotational Abrasion device has been introduced, and the abrasion resistance of concrete pavements with different textures was investigated using Rotational Abrasion Test as well as Wide Wheel Abrasion Test. The findings are summarized as follows:

1. The results of Rotational Abrasion Test show good conformities with those of the Wide Wheel Abrasion Test, indicating that the former test can be used as a reliable method for measuring concrete pavement abrasion susceptibility.
2. The texture types have the following descending sequence with respect to the abrasion rate: G, Per.B, Par.B, T.D, B.D, and N.T. However, the weight loss of type G texture is a result of edge breakage as well as abrasion.
3. The results of type G and B.D textures, measured by the mentioned tests, showed some discrepancies which are mostly due to the limited contact area in Wide Wheel Abrasion Test.
4. Rotational Abrasion Test results indicate that abrasion rates of concrete pavements decrease as loading proceeds. Surface poor curing and loss of integrity due to texturing are identified as root causes of this issue.
5. Grooved samples underwent significantly more abrasion compared to samples with different textures. Although the abrasion rate of these samples decrease through loading, as others, after a specific number of wheel passage (400 loading iteration), it approaches a constant value. This is not only a result of abrasion process, but also fracture of grooves edges. To prevent the fracture of groove edges, evaluations need to be done on width and depth of the grooves, before being

implemented on the pavement surface.

6. Negative textures are less likely to be engaged with external objects; therefore, Wide Wheel Abrasion Test, considering its limited wheel contact area, cannot yield reliable results. The rotational abrasion test on the other hand, is indeed simulating the realistic loading conditions in field, thus, the negative texture results are quite reliable.

## ACKNOWLEDGMENT

Authors wish to express their gratitude to Dr. Dibae, Mr. Habibi and Mr. Gharashi for their assistance.

## REFERENCES

- Adewuyi, A.P., Sulaiman, I.A. and Akinyele, J.O. (2017). "Compressive strength and abrasion resistance of concretes under varying exposure conditions", *Open Journal of Civil Engineering*, 7(01), 82.
- Ahamed, M.A. and Tighe, S.L. (2008). "Concrete pavement surface textures and multivariables frictional performance analysis: A North American case study", *Canadian Journal of Civil Engineering*, 35(7), 727-738.
- American Concrete Institute, Committee 211, (1977). *Recommended practice for selecting proportions for normal and heavyweight concrete (ACI 211.1-77)*, Detroit: The Institute.
- Ardani, A.A. (2006). *Implementation of proven PCCP practices in Colorado (No. CDOT-DTD-R-2006-9)*.
- ASTM C1138M-12, (2012), *Standard test method for abrasion resistance of concrete (Underwater method)*, ASTM International, West Conshohocken, PA, [www.astm.org](http://www.astm.org),
- ASTM C944 / C944M-12, (2012), *Standard test method for abrasion resistance of concrete or mortar surfaces by the rotating-cutter method*, ASTM International, West Conshohocken, PA, [www.astm.org](http://www.astm.org)
- ASTM G40-15, (2015), *Standard terminology relating to wear and erosion*, ASTM International, West Conshohocken, PA, [www.astm.org](http://www.astm.org)
- China National Standard, (1997). *Test method for abrasion resistance of concrete and its products (Ball bearing method)*, GB/T 16925-1997
- García, A., Castro-Fresno, D., Polanco, J.A. and Thomas, C. (2012). "Abrasive wear evolution in

- concrete pavements”, *Road Materials and Pavement Design*, 13(3), 534-548.
- Ghanbari, A., Hamidi, A. and Abdolazadeh, N. (2013). “A study of the rockfill material behavior in large-scale tests”, *Civil Engineering Infrastructures Journal*, 46(2), 125-143.
- Gonzalez, M., de Oliveira Lima, A. and Tighe, S. (2014). “Nanocrete for rigid pavements: Abrasion response and impact on friction”, *Transportation Research Record*, 2441(1), 28-37.
- Hall, J.W., Smith, K.L. and Littleton, P.C. (2009). *Texturing of concrete pavements*, Vol. 634, Transportation Research Board.
- Horszczaruk, E. (2005). “Abrasion resistance of high-strength concrete in hydraulic structures”, *Wear*, 259(1-6), 62-69.
- Horszczaruk, E. (2008). “Mathematical model of abrasive wear of high performance concrete”, *Wear*, 264(1-2), 113-118.
- Iranian Legal Medical Organization. (2017). <http://www.lmo.ir/> (in Persian).
- Jalal Kamali, M.H., Monajjem, M.S. and Ayubirad, M.S. (2013). “Studying the effect of spiral curves and intersection angle, on the accident ratios in two-lane rural highways in Iran”, *Promet-Traffic and Transportation*, 25(4), 343-348.
- Jalal Kamali, M.H. (2012). “The feasibility of using transition curve in road design to improve safety”, M.Sc. Thesis, Shahid Chamran University of Ahvaz, (In Persian).
- Li, H., Zhang, M.H. and Ou, J.P. (2006). “Abrasion resistance of concrete containing nano-particles for pavement”, *Wear*, 260(11-12), 1262-1266.
- Purwanto, P. and Priastiwi, Y.A. (2008). “Testing of concrete paving blocks the BS EN 1338: 2003 British and European standard code”, *Teknik*, 29(2), 80-84.
- Rasouli, M.R., Nouri, M., Zarei, M.R., Saadat, S. and Rahimi-Movaghar, V. (2008). “Comparison of road traffic fatalities and injuries in Iran with other countries”, *Chinese Journal of Traumatology (English Edition)*, 11(3), 131-134.
- Siddique, R. (2013). “Compressive strength, water absorption, sorptivity, abrasion resistance and permeability of self-compacting concrete containing coal bottom ash”, *Construction and Building Materials*, 47, 1444-1450.
- ASTM C779 / C779M-12, (2012). *Standard test method for abrasion resistance of horizontal concrete surfaces*, ASTM International, West Conshohocken, PA, [www.astm.org](http://www.astm.org).
- Wallman, C.G. and Åström, H. (2001). *Friction measurement methods and the correlation between road friction and traffic safety: A literature review*. Statens väg-och Transport for Sknings Institute.
- Wang, H. and Liang, R.Y. (2014). “Predicting field performance of skid resistance of asphalt concrete pavement”, In: *Pavement Materials, Structures, and Performance*, pp. 296-305.
- Wu, Z., King, B., Abadie, C. and Zhang, Z. (2012). “Development of design procedure to predict asphalt pavement skid resistance”, *Transportation Research Record*, 2306(1), 161-170.
- Xiao, J., Kulakowski, B. and El-Gindy, M. (2000). “Prediction of risk of wet-pavement accidents: Fuzzy Logic model”, *Transportation Research Record*, 1717(1), 28-36.
- Yoshitake, I., Ueno, S., Ushio, Y., Arano, H. and Fukumoto, S. (2016). “Abrasion and skid resistance of recyclable fly ash concrete pavement made with limestone aggregate”, *Construction and Building Materials*, 112, 440-446.